

Alternate time scale in multimode lasers

Kenju Otsuka

NTT Basic Research Laboratories, Musashino-shi, Tokyo 180, Japan

Paul Mandel

Université Libre de Bruxelles, Campus Plaine, Code Postal 231, 1050 Bruxelles, Belgium

S. Bielawski, D. Derozier, and P. Glorieux

Laboratoire de Spectroscopie Hertzienne, Université de Lille I, F-59655 Villeneuve d'Ascq, CEDEX, France

(Received 28 October 1991)

We analyze the intensity fluctuation of multimode lasers by extending the linear-response theory of McCumber for single-mode lasers. In the two-mode case, we prove analytically that the rate equations allow for an additional dynamical oscillation frequency associated with the antiphase motion. This explains the self-organized collective behavior of two-mode lasers, i.e., that the total output behaves just like a single-mode laser. The linear stability predicts the scaling law for this time scale, which results quite generally through cross-saturation dynamics of population inversion. Experimental results in two different laser systems confirm these predictions.

PACS number(s): 42.55.Rz, 42.50.Fx

It has been known that multimode lasers exhibit complicated behaviors from the early dates of experimental observation. Complex multimode laser dynamics have recently been revisited as an intriguing subject for the study of nonlinear dynamics in optical systems. The issue of intensity fluctuation in the output of lasers has a long history. McCumber predicted a noise peak in power spectra corresponding to relaxation oscillations in single-mode class-B lasers, in which polarization dynamics can be adiabatically eliminated, on the basis of linear-response theory in 1966 [1]. On the other hand, Tang, Stutz, and deMars pointed out self-organized *collective behavior* in transient oscillations of two-mode lasers, which implies that the total output behaves just like a single-mode laser. In short, they showed that the intensities of the individual modes show irregular spiking but the total output intensity could still exhibit a regular damped relaxation oscillation much like that of the single-mode laser on the basis of numerical simulations in 1963 [2]. They found that in some parameter regions that the relaxation oscillations in the two modes tend to oscillate in opposite phase—the maxima of one mode tend to coincide with the minima of the other. However, this does not insure the collective behavior and its physical interpretation is still an open question. Recently, similar collective behaviors have been observed in intracavity second-harmonic generation in multimode lasers [3] and in deeply modulated multimode lasers [4] even in pulsating regimes. This collective behavior is considered to be basic to the understanding of complex dynamics in multimode lasers. The purpose of this Brief Report is twofold: to extend the McCumber theory to multimode lasers for predicting time scales of intensity fluctuations and to identify the mechanism responsible for the collective behavior in multimode lasers. We report on two models and corresponding experiments that support the

theoretical predictions.

We begin by studying the Tang, Stutz, and deMars equations [2] for a two-mode laser, including the cross-saturation effect due to spatial hole burning. The rate equations are

$$\begin{aligned}\frac{dn_0}{dt} &= w - n_0 - I_1(2n_0 - n_1)/2 - \gamma I_2(2n_0 - n_2)/2, \\ \frac{dn_1}{dt} &= n_0 I_1 - n_1(1 + I_1 + \gamma I_2), \\ \frac{dn_2}{dt} &= \gamma n_0 I_2 - n_2(1 + I_1 + \gamma I_2), \\ \frac{dI_1}{dt} &= \kappa I_1[(2n_0 - n_1)/2 - 1], \\ \frac{dI_2}{dt} &= \kappa I_2[\gamma(2n_0 - n_1)/2 - 1].\end{aligned}\quad (1)$$

I_j is the average photon number in mode j and n_0 the space average of the population inversion, while n_j is defined as

$$n_j = (2/L) \int_0^L n(x, t) \cos(2k_j x) dx,$$

where k_j is the wave number of mode j and L is the length of the laser cavity, which is filled with the active medium. Thus, the dynamics of n_1 and n_2 explicitly takes into account the grating effects of standing-mode patterns in the cavity. The optical pump parameter w is scaled to the first laser threshold, γ is the gain ratio of the two modes, and κ is the relative photon lifetime. Time and κ are scaled to the population lifetime.

The crucial role in the dynamics that we shall analyze is played by the ratio $\beta_{1,2}$ of the cross-saturation parameter over the self-saturation parameter. In our model,

these coefficients are pump-dependent functions, which results from the fact that the spatial hole depth changes with pump intensity. They decrease with an increase of the pump and approach $\beta_1 = \gamma/2$ and $\beta_2 = \frac{1}{2}$ in the limit of $w \gg 1$. For ordinary solid-state lasers, κ ranges between 10^3 and 10^6 . The main point is that whatever precise value of κ is imposed by experimental considerations, it can be used as a large parameter in terms of which asymptotic analyses can be performed.

Equations (1) have three steady-state solutions: (i) the nonlasing solution ($I_1 = I_2 = 0$); (ii) the single-mode solution ($I_1 \neq 0, I_2 = 0$), which bifurcates from the nonlasing mode at the laser first threshold $w_{th} = 1$; and (iii) the two-mode solution, in which both I_1 and I_2 have nonzero steady solutions. This two-mode solution exists for

$$w \geq w_c = (2\gamma^2 - 4\gamma + 1) / [\gamma(1 - 2\gamma)],$$

if and only if $\gamma \geq \frac{1}{2}$.

A linear stability analysis of the trivial solution indicates that it is stable for $w < 1$. The single-mode solution is stable for $1 < w < w_c$. For large values of κ , the relaxation towards the steady state is characterized by damped oscillations. The oscillation frequency ω_R , in the time scale t , was first derived by McCumber [1] and is given by

$$\omega_R^2 = \kappa \Omega_R^2 = \kappa I_1 (3n_0/2 - n_1) = \kappa I_1 (4 - n_0) / 2 \propto \kappa (w - 1). \quad (2)$$

Linear stability of the two-mode solution above w_c is easily analyzed in the limit $\kappa \gg 1$. It yields five roots. Four roots scale like $\kappa^{1/2}$. To dominant order in κ , they are imaginary and define two dynamical frequencies, ω_R and ω_L , given by

$$\omega_R^2 = \kappa I_1 (4 - n_0) / 2, \quad \Omega_L^2 = \frac{I_1 I_2}{\Omega_R^2} \varphi(\gamma, n_0) < \Omega_R^2, \quad (3)$$

$$\omega_L^2 = \kappa \Omega_L^2, \quad \varphi(\gamma, n_0) = -(\gamma - 1)^2 + \gamma n_0 (1 + \gamma - 3\gamma n_0 / 4). \quad (4)$$

From this result, the following scaling laws are derived:

$$\omega_R^2 \propto \kappa (w - w_{th}), \quad \omega_L^2 \propto \kappa (w - w_c). \quad (5)$$

After analyzing two other models from two-mode lasers [5], we found that relation (3), and therefore scaling laws (5), hold quite generally and that only the function φ , which is an $O(1)$ function, is model dependent. The fifth root of the linear stability analysis is an $O(1)$ real decay rate.

To understand the relation between the relaxation oscillation and the low-frequency motions in an exaggerated scale, we first show large signal transient behaviors. The temporal evolutions of the modal and the total intensities obtained by integrating Eqs. (1) are shown in Fig. 1. In this figure, the faster oscillation component corresponds to ω_R and the slow oscillation component, which is evident for I_2 and is also indicated by a dashed curve for I_1 , corresponds to ω_L . The low-frequency motions

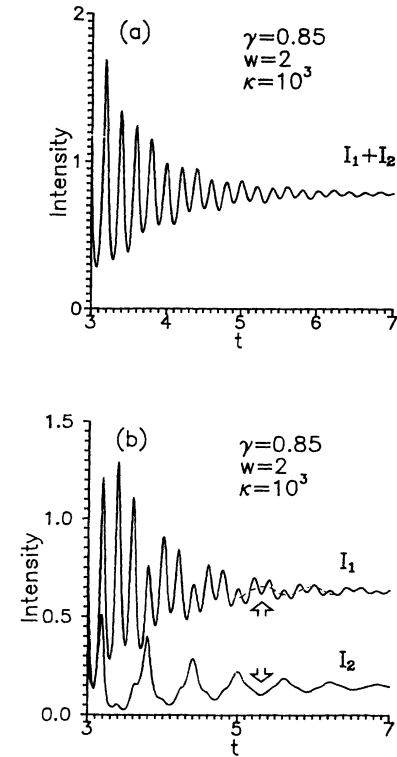


FIG. 1. Transient behavior of the intensities of a two-mode laser: (a) total intensity and (b) partial intensities.

have opposite phases for the two modes. Therefore, this motion can be referred to as the antiphase motion. This is the origin of the total intensity in Fig. 1(a), showing a regular relaxation oscillation, i.e., *collective behavior*. Therefore, we can easily expect that the total output possesses only a single power spectrum peak at ω_R , while the modal output shows an additional peak at ω_L , as shown in Fig. 2.

To confirm the existence of two intrinsic frequencies of intensity fluctuations derived from the linear stability analysis, we show the measured noise power spectra of a continuously oscillating two-mode LiNdP₄O₁₂ (LNP)

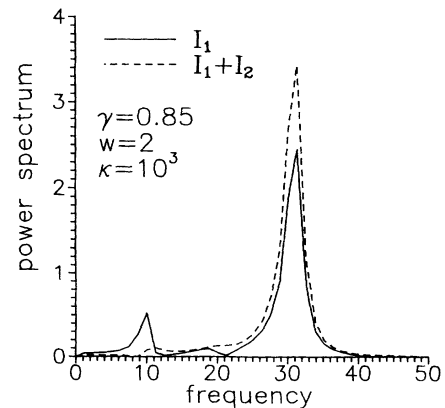


FIG. 2. Power spectra of the strong mode I_1 and the total intensity, which correspond to Fig. 1.

laser, whose dynamics are governed by Eqs. (1) [6]. The result is shown in Fig. 3, where these noises appear through a small pump fluctuation. It is apparent that the total output shows a single ω_R peak, while the modal output exhibits additional ω_L peaks. This implies that the antiphase characteristics exist even in the vicinity of stationary states.

Next, let us consider another laser system, i.e., a Nd^{3+} -doped optical fiber laser (OFL) pumped by a diode laser. When operated well above threshold, such a laser is highly multimode. In spite of that, the dynamical behavior of the OFL presents some extremely simple collective features. When the pump power is increased from zero, the laser exhibits a first threshold above which laser radiation is emitted in a linear polarization state in a wavelength band that broadens as the pump is increased. Above a second threshold, radiation is also emitted in the orthogonal polarization, first in a narrow wavelength region, and at higher pump power, in a wider range up to 50 cm^{-1} . The relative position of the two thresholds can be adjusted by rotating the pump polarization or changing the stress applied to the fiber. These two linear polar-

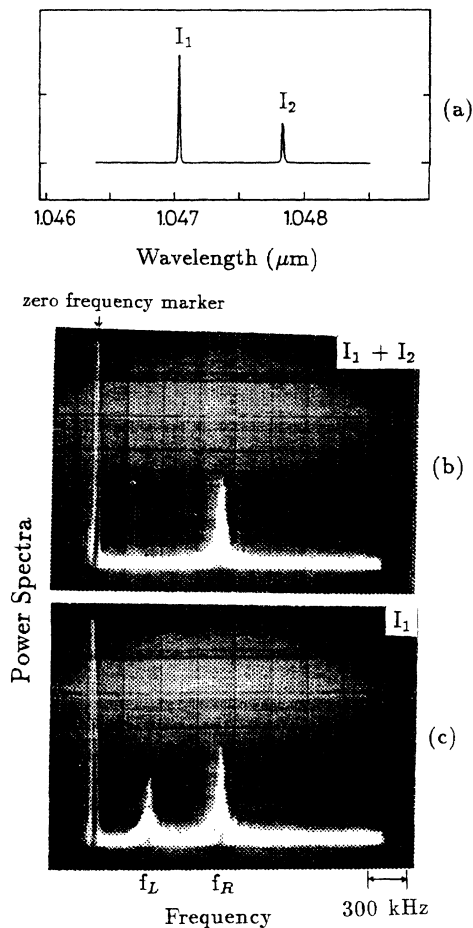


FIG. 3. (a) Oscillation mode spectrum of a $300\text{-}\mu\text{m}$ -thick LNP laser pumped by an Ar laser; (b) noise power spectrum for the total intensity; (c) noise power spectrum for I_1 . $\omega = 7.5$ and $\kappa = 10^5$.

ization states are the eigenstates of the polarization for the cavity in the presence of the small stress-induced birefringence due to bending of the 5-m -long fiber.

The response of this laser to pump modulation has been investigated in both the sinusoidal and the square pulse regimes. The output intensity is analyzed simultaneously in both of the linear polarization states discussed above and the total intensity has also been recorded. The response to small sinusoidal modulation exhibits two resonances, a strong one at the frequency ω_R of the usual relaxation oscillations and a weaker one at a low frequency ω_L which is not related in a simple way to ω_R . The low-frequency ω_L varies with the stress-induced birefringence, but it exists even in the degenerate situation in which both thresholds coincide.

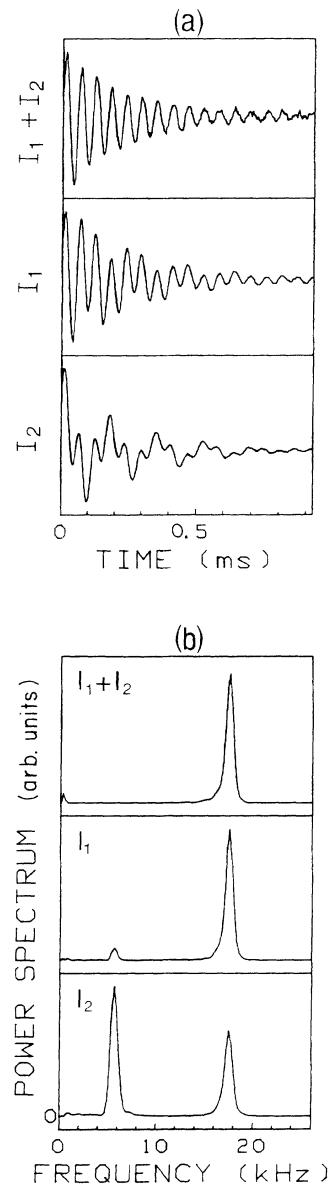


FIG. 4. Experimental recordings of the response of the OFL to pulse excitation; (a) refers to the intensities and (b) refers to the corresponding power spectra.

The dynamical properties of the two modes are more clearly visible when the transient response of the laser to a pulsed perturbation of the steady state is observed. Qualitatively different signals are obtained depending on the observed quantities. The intensities I_1 and I_2 along both linear polarization axes exhibit simultaneously slow and fast relaxation oscillations, while the total intensity, which is recorded on an independent detector, shows only the fast frequency component. As the total intensity is just the sum of I_1 and I_2 , this indicates that the low-frequency components of I_1 and I_2 destructively interfere and consequently are in antiphase. Such a behavior is illustrated in Fig. 4(a) where the OFL measured intensities I_1 , I_2 , and $I_1 + I_2$ have been plotted. Correspondingly, in Fig. 4(b) we have plotted the power spectra of I_1 , I_2 , and $I_1 + I_2$. There is no evidence of a low-frequency oscillation in the power spectrum of the total intensity, while the polarization selected intensity displays such a component near 6 kHz.

The relation between ω_R^2 and ω_L^2 versus the pump intensity is shown in Fig. 5. As for monomode lasers, the frequency of the relaxation oscillations tends to zero as the first threshold is approached. The low-frequency oscillation exists only above the second threshold, i.e., where both polarization clusters are oscillating. Figure 5 illustrates the excellent agreement with the proposed scaling law over the entire attainable range of experimental parameters.

The double resonance to weak modulations and the transient behavior featuring antiphase motions, together with the scaling law shown above, imply that, surprisingly, hundreds of modes form clusters in two subsets, one associated with each polarization direction, and each cluster may be described as one mode. (A similar clustering of many oscillating modes was reported for dual-polarization LNP lasers, in which each polarization behaves like a single-mode FM laser [7].)

To confirm this fact, numerical simulations were also undertaken on a model designed to describe the OFL as a system of two lasers sharing the same cavity and coupled by cross-saturation terms:

$$\begin{aligned} \frac{dn_j}{dt} &= w_j - (1 + I_j + \beta I_{3-j})n_j, \\ \frac{dI_j}{dt} &= \kappa[(n_j + \beta n_{3-j} - 1)I_j + a(n_j + \beta n_{3-j})], \\ & j = 1 \text{ or } 2 \quad (6) \end{aligned}$$

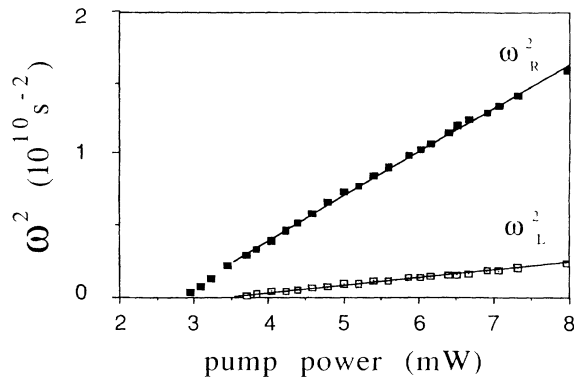


FIG. 5. Dependence of the oscillation frequencies of the system vs the pump power. The first threshold is at 3 mW and the threshold for bimode operation at 3.5 mW. Here, oscillation frequencies ω_R and ω_L are measured frequencies.

where β is the cross-saturation parameter and a is associated with spontaneous emission. Other notations are the same as Eq. (1). This model has common features with the two-mode model given by Eqs. (1) and with the experiment, namely, a low-frequency relaxation oscillation with the scaling law (5) and antiphase behavior for the low-frequency response to pulsed perturbation of the steady state in the region of bimode oscillation.

In conclusion, an additional time-scale intensity fluctuation in two-mode lasers has been predicted analytically. This time scale, featuring antiphase motion, is shown to appear quite generally through the cross-saturation dynamics of population inversion. The scaling law and antiphase motion, which is the origin of the self-organized collective behavior, have been confirmed in two different laser systems. The theoretical analysis has been extended to the N -mode problem and a detailed presentation of this generalization is included in Ref. [8].

K. Otsuka is indebted to the Interuniversity attraction pole program of the Belgian government for supporting him in Brussels where most of this research was carried out. P. Mandel acknowledges partial support of the Fonds National de la Recherche Scientifique. The Laboratoire de Spectroscopie Hertzienne is "associé au CNRS."

- [1] D. E. McCumber, *Phys. Rev.* **141**, 306 (1966).
 [2] C. L. Tang, H. Statz, and G. deMars, *J. Appl. Phys.* **34**, 2289 (1963).
 [3] K. Wiesenfeld, C. Bracikowski, G. James, and R. Roy, *Phys. Rev. Lett.* **65**, 1749 (1990).
 [4] K. Otsuka, *Phys. Rev. Lett.* **67**, 1090 (1991).

- [5] K. Otsuka and J.-L. Chern, *Phys. Rev. A* **45**, 5052 (1992), and the model described by Eq. (6) later.
 [6] K. Otsuka, *Appl. Opt.* **21**, 744 (1982).
 [7] K. Otsuka, K. Kubodera, and J. Nakano, *IEEE J. Quantum Electron.* **13**, 398 (1977).
 [8] P. Mandel, M. Georgiou, and K. Otsuka (unpublished).

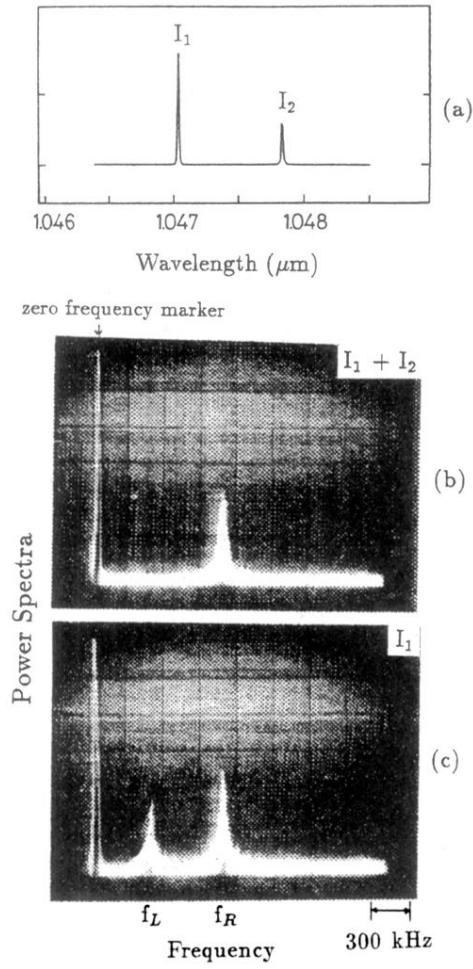


FIG. 3. (a) Oscillation mode spectrum of a 300- μm -thick LNP laser pumped by an Ar laser; (b) noise power spectrum for the total intensity; (c) noise power spectrum for I_1 . $w=7.5$ and $\kappa=10^5$.